Journal of Membrane Science 601 (2020) 117842

Contents lists available at ScienceDirect

Journal of Membrane Science

journal homepage: http://www.elsevier.com/locate/memsci

Superhydrophobic-superoleophilic SiC membranes with micro-nano hierarchical structures for high-efficient water-in-oil emulsion separation

Yibin Wei, Zixuan Xie, Hong Qi *

State Key Laboratory of Materials-Oriented Chemical Engineering, Membrane Science and Technology Research Center, Nanjing Tech University, Nanjing, 210009, China

ARTICLE INFO

Keywords:
Superhydrophobic
SiC
Ceramic membrane
ZnO
Oil-water separation

ABSTRACT

Superhydrophobic-superoleophilic ceramic membranes with chemical, thermal and mechanical robustness are promising for efficient water-in-oil emulsion separation. Here, we report a facile approach to fabricate superhydrophobic-superoleophilic SiC membranes via ZnO nanosphere (NS) deposition and n-octyltriethoxysilane surface grafting. ZnO NSs were grown onto SiC grains by chemical solution deposition method to form micro-nano hierarchical structures for the membrane surfaces. By tuning the precursor concentration, the surface structures of SiC-25, SiC-50 and SiC-75 membranes ($C(Zn^{2+})$ = 25, 50 and 75 mM) were tailored with the increasing density of ZnO NSs. We found that the surfaces of SiC-50 and SiC-75 membrane were superhydrophobic-superoleophilic. Compared with pristine and simply grafted SiC membranes, the three SiC membranes with ZnO NS and grafting modification displayed excellent water rejection (>99.0%) and superior oil flux. The SiC-50 membrane displayed the optimal performance with steady-state flux was up to ~1000 L m^{-2} h^{-1} under 1 bar for 500 ppm water-in-hexane emulsion. The effects of surface structure and wettability on water-in-oil emulsion separation performance is revealed. We also confirmed the stability of the superhydrophobicity for the SiC-75 membrane. This work offers new insights into constructing robust superhydrophobic-superoleophilic ceramic membranes for high-performance water removal from oil products.

1. Introduction

High-efficient separation of oil-water mixtures has been considered as an urgent need for many agricultural and industrial processes associated with energy, water and environmental securities [1,2]. Among various types of oil-water mixtures, emulsified oil-water mixtures are regarded as the most challenging to be separated [3]. Oil-water emulsions can be divided into oil-in-water (o/w) and water-in-oil (w/o) emulsions according to the dispersed phase and the continuous phase [4]. Surfactant-stabilized oil-water emulsions own low interfacial tension between the two phases leading to the formation of stable and small droplets, which makes them even difficult for separation [5].

As an advanced separation and purification technology, membrane-based technology has been extensively applied in oil-water separation due to its significant technical and economical superiorities such as low energy cost, ease for continuous operation, and small footprint [6]. However, severe flux decline exists in nearly all oil-water separation processes, especially for oil-water emulsion separation [7]. In addition, the potential corrosion of oils, possibly high temperature working circumstances and high viscosity of oils should be also concerned in practical applications, which requires membrane materials to be chemically, thermally and mechanically robust for long-term use [8]. Therefore, the development of robust and high-flux membrane materials is the key to achieve high-efficient oil-water separation.

Ceramic membranes own excellent reliability for industrial fluids separation under harsh conditions [9] and there is a growing tendency employing ceramic membranes for oil-water separation, especially for oil field and refinery produced water treatment in the recent years [10]. Although the commercial ceramic membrane materials are robust enough, they are usually not suitable for w/o emulsions separation because they are mainly made of metal oxides displaying strong hydrophilicity and the wettability leads to poor oil flux for such applications [11]. For improving the efficiency in w/o emulsion separation, ceramic membranes are desired to be hydrophobic-oleophilic for avoiding pore blockage by water [12]. However, since ceramic membranes are intrinsically hydrophilic, conferring hydrophobicity on their surfaces yet maintaining ceramic merits remains challenging.

Surface grafting with silane reagents is the most widely used

* Corresponding author.
E-mail address: hqi@njtech.edu.cn (H. Qi).

https://doi.org/10.1016/j.memsci.2020.117842
Received 4 November 2019; Received in revised form 10 January 2020; Accepted 11 January 2020
Available online 13 January 2020

approach to shift ceramic membranes from hydrophilic to hydrophobic [13]. Silane molecules usually consist of one Si atom connected with four functional groups, SiX_4. Silane reagents can be activated in organic solvents to form active silanol species, which are easily chemisorbed on the ceramic membrane surfaces. Moreover, the excess Si–OH of the chemisorbed silane can further link with the adjacent silane molecules through the Si–O–Si bonds. The chemical bonding and intermolecular interaction are very strong which imparts the hydrophobicity for ceramic membranes [14]. The post-modification process is very simple and effective to change the surface chemical composition of ceramic membranes and lower their surface energy [15,16]. However, many studies pointed out that the ceramic membranes could acquire a relatively high hydrophobicity after facilely grafting with silane reagents but their surfaces still could not reach the superhydrophobic state (i.e. water contact angle (WCA) $> 150°$ and sliding angle $< 10°$) [17]. Consequently, the saline-modified ceramic membranes generally displayed very limited improvement in separation efficiency for w/o emulsions compared with its pristine form [18]. This could be attributed to the insufficient water-repellency of the ceramic membrane surface that water droplets could still contact and block the pores and trigger oil flux decline [19].

Inspired by many water-repellency plants and animals in nature (e.g., lotus leaf, legs of the water strider, and the eyes of mosquitos), superhydrophobic interfacial materials have recently attracted increasing attention in many fields such as self-cleaning, anticorrosion, antifogging, anti-icing and oil-water separation [20,21]. Superhydrophobicity not only endows polymeric or metal mesh-based membranes with outstanding water-repellency for oil-water separation but also challenges the traditional understandings of membrane flux and selectivity [22,23]. However, the reported superhydrophobic polymeric membranes may also suffer from degradation under harsh conditions and the metal mesh-based membranes are not suitable for large-scale continuous operation. Therefore, designing and fabrication of superhydrophobicity on intrinsically robust ceramic membranes is extremely promising for practical w/o emulsions separation. To the best of our knowledge, there are very few reports on the fabrication of superhydrophobic ceramic membranes materials [24–27] and their applications in w/o emulsion separation are also scarce.

Generally, chemical composition and surface roughness (structure) are two essential factors to construct superhydrophobic surfaces. To prepare a superhydrophobic ceramic membrane, a special surface structure with sufficient roughness and low surface energy is required [28,29]. In this work, zinc oxide nanospheres (ZnO NSs) were first deposited onto the SiC membrane surface through a reliable chemical solution deposition method. The NSs were grown onto the microscale SiC grains to form micro-nano hierarchical structures. By tuning the concentration of Zn^{2+} during the chemical solution deposition reaction, the ZnO–SiC composite structures were finely tailored by the density of ZnO NSs. Using n-octyltriethoxysilane as grafting reagent, the resulting ZnO–SiC composite structures were then post-treated to modify their surface chemical compositions. The relationship between surface structure and wettability of the corresponding membranes were well elucidated by various characterization techniques. The effects of the structures and their wettability on the consequent w/o emulsions separation performance were investigated.

2. Experimental

2.1. Materials

Zinc nitrate hexahydrate ($Zn(NO_3)_2{\cdot}6H_2O$, $\geq$ 99.8%) and Span-80 were purchased from Sinopharm Group Co. Ltd (China). Potassium permanganate ($KMnO_4$, $\geq$99.8%), triethanolamine (TEA, $\geq$ 78%), tert-butanol (*t*-butanol) and ammonium hydroxide ($NH_3{\cdot}H_2O$, 26%) were supplied by Shanghai Lingfeng Chemical Reagent Co. Ltd (China). Diiodomethane and n-octyltriethoxysilane ($C_{14}H_{32}O_3Si$, 97%) were obtained from Shanghai Aladdin Biochemical Technology Co., Ltd (China). Ethylene glycol and hexane were obtained from Shanghai Sihewei Chemical Co., Ltd (China). All chemicals were used as received without further purification. Disc-type microfiltration (MF) SiC membranes (diameter: 41 mm; thickness: 2 mm; average pore size: 250 nm; porosity: 21.3%; bending strength: 86.5 MPa) were provided by Nanjing Hongyi Ceramic Membrane Co. Ltd., China. The pore size distribution and pure water flux of the pristine SiC membrane (SiC–P) varying with transmembrane pressures could be found in Fig. S1. Deionized (DI) water (conductivity < 5 μS·cm^{-1} at 25 °C) manufactured by Membrane Science and Technology Research Center, State Key Laboratory of Materials-Oriented Chemical Engineering was used throughout this study.

2.2. ZnO nanospheres (NSs) deposition

A reliable and facile chemical solution deposition approach was used to deposit ZnO NSs on SiC membrane surfaces [30,31]. Firstly, the SiC membranes were immersed in a polytetrafluoroethylene (PTFE) beaker filled with a fresh $KMnO_4$ aqueous solution for surface pretreatment. The solution was prepared with 0.3161 g $KMnO_4$ in 40 mL DI water containing 0.1 mL t-butanol. The surface pretreatment process was conducted at room temperature with stirring for 1 h. Then, the $KMnO_4$-treated SiC membranes were intensively cleaned using DI water in an ultrasonic bath for several times for avoiding homogeneous nucleation in the deposition process from Mn-containing contaminants.

For ZnO NSs deposition, ZnO deposition solutions with Zn^{2+} concentrations of 25 mM, 50 mM and 75 mM were prepared, respectively. Briefly, a certain amount of $Zn(NO_3)_2{\cdot}6H_2O$ were first dissolved in 35 mL DI water to prepare Zn^{2+} aqueous solution, then 4 mL TEA and 1 mL $NH_3{\cdot}H_2O$ were added for the preparation of ZnO deposition solution. Next, the surface activated SiC membranes were put into the ZnO deposition solution in a PTFE beaker. Followed by this, the PTFE beaker was closed and placed in an oil bath at 96 °C for 40 min. After deposition, the ZnO-deposited membrane was rinsed with plenty of DI water for several times prior to drying in an oven at 100 °C overnight.

2.3. Surface grafting with n-octyltriethoxysilane

The ZnO-deposited SiC membranes were then grafted with n-octyltriethoxysilane for the hydrophobic transition. A 0.2 mol/L grafting solution was prepared by dissolving 6.5 mL n-octyltriethoxysilane in 100 mL ethanol anhydrous. The ZnO-deposited SiC membranes were immersed in the solution at 40 °C for 12 h. After the grafting process, the membranes were washed with ethanol/DI water mixture (v/v = 1:1) and DI water for several times and dried in an oven at 80 °C for 5 h before use. The finally grafted SiC membranes that prepared by Zn^{2+} concentrations of 25 mM, 50 mM and 75 mM were noted as SiC-25, SiC-50, SiC-75, accordingly. For comparison, the SiC–P membrane was also grafted with n-octyltriethoxysilane in the same procedure in this work and the directly grafted SiC membrane was noted as SiC-G. The above-mentioned membrane preparation procedure is simply presented in Fig. 1.

2.4. Characterization

A Hitachi SU8000 scanning electron microscope equipped with electron dispersive spectrometry (SEM-EDS) was used to image surface morphologies and analyze elemental information of membranes. Membrane surface roughness was measured using a surface profiler (Bruker, Contour, GT-K) with a scan size of 94 × 130 μm. An X-ray photoelectron spectrometer (XPS) (Thermo Fisher, ESCALAB 250Xi) was used for the quantitative elemental analysis of membrane surfaces. The X-ray source is monochromated Al Kα ($h\nu$ = 1486.6 eV). The binding energies were calibrated with reference to C1s at 284.8 eV for adventitious hydrocarbon contamination. The spot size was 650 μm and scans were

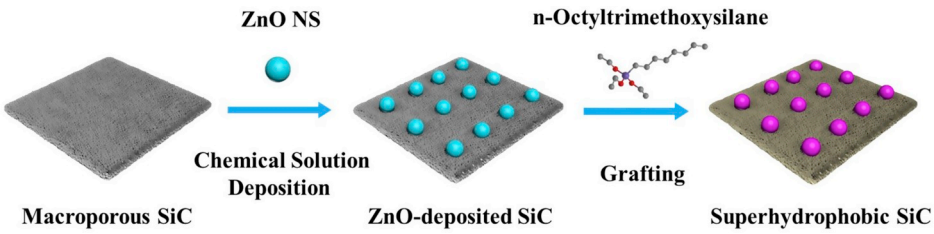

Fig. 1. Schematic illustration for the preparation process of superhydrophobic SiC membranes.

repeated 10 times.

The pore size distribution of the pristine SiC membrane was measured by a MF membrane porometer (PSDA-20, Nanjing GaoQ functional material Co., Ltd China). The surface wettability of membranes was analyzed by a contact angle (CA) goniometer (A-100P, MAIST, Ningbo Haishumaishi). Static or dynamic CAs for membrane surfaces were recorded by dropping 5 μL liquid (water or oil) droplets on the surfaces. The CA values were determined by repeating three measurements. The surface free energies of membranes were calculated based on Wu's Method [32] and Van Oss' Method [33]. Diiodomethane, ethylene glycol and DI water were used as testing liquids and the CAs on membrane surfaces were recorded.

2.5. Membrane filtration test

The water-in-oil (w/o) emulsion separation performance of membranes was evaluated by a home-made cross-flow filtration configuration (Fig. S2). The effective area of the membrane surface is 11.04 cm^2. All experiments were conducted at 25 °C with a constant transmembrane pressure of 1 bar. The feed w/o emulsions were 500 ppm, 1000 ppm and 2000 ppm water-in-hexane emulsions, and Span 80 was used as the emulsifier. The mass ratio of water and Span was 10:1. For example, 0.1 g Span 80 and 1 g DI water were added into 2 L hexane first and the obtained mixture was then stirred by a high-shear dispersion emulsifying machine (Shanghai FLUKO) at a speed of 3000 rpm for 15 min to obtain well-dispersed 500 ppm w/o emulsion. The permeated oil was continuously collected and monitored by a glass cylinder. The oil flux is calculated according to Eq. (1):

$$J = \frac{V}{A \times t} \tag{1}$$

where J is the flux ($L \cdot m^{-2} \cdot h^{-1}$), V is the volume of collected oil (L), A is the membrane effective area (m^2), and t is the permeation time (h). The pure water flux of the pristine SiC membranes was obtained similarly using the same configuration.

The rejection (R) efficiency is calculated using Eq. (2):

$$R = \left(1 - \frac{C_p}{C_f}\right) \times 100\ \% \tag{2}$$

where C_p and C_f are the water concentrations of the permeate and feed solutions, respectively. The feed w/o emulsions and the permeated solutions were analyzed using optical microscopy equipped with a digital camera (Leica DMi8). The size distribution of water droplets in the feed and the permeate were measured by dynamic light scattering (DLS, Malvern Nano ZS90).

3. Results and discussion

3.1. Morphological and chemical characterization

Fig. 2 shows the surface morphologies of SiC–P, SiC-G, SiC-25, SiC-50 and SiC-75 membranes observed using SEM. The surface morphologies of the pristine and the silane-grafted SiC membranes were similar indicating that the silane grafting could not generate a visible layer onto the SiC membrane surface under SEM observation (Fig. 2a–b). Similar results were also found by other researchers that silane could only form a thin self-assembled monolayer (SAM) with the thickness of a few nanometers [18]. We observed that ZnO nanospheres (NSs) with the diameter of 300–500 nm were uniformly deposited on the micrometer-sized SiC grains and the density of ZnO NSs for the three ZnO-deposited SiC membranes increased with the increase of Zn^{2+}

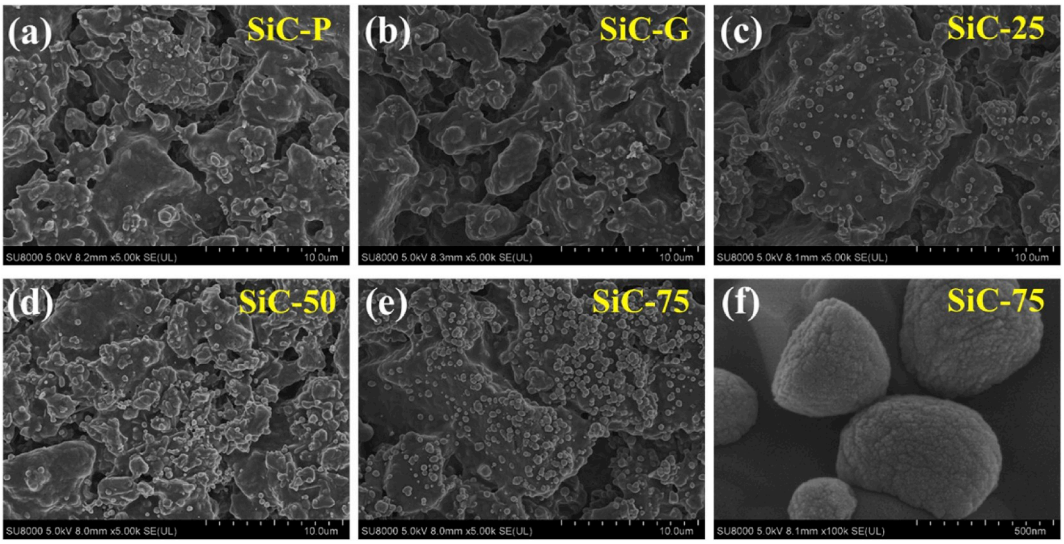

Fig. 2. SEM images of (a) SiC–P, (b) SiC-G, (c) SiC-25, (d) SiC-50, (e) SiC-75 membrane surfaces, and (f) ZnO NSs on SiC-75 membrane surface observed under high resolution.

concentration (Fig. 2c–f). The EDS analysis was conducted for the SiC-75 membrane surface to understand the elemental distribution of the ZnO-deposited SiC membranes (Fig. 3). The elemental maps further demonstrated that the ZnO NSs were grown onto SiC grains and micro-nano hierarchical structures were formed on the SiC membrane surfaces.

Fig. 4 shows the three-dimensional surface morphological images and the corresponding roughness parameters of the SiC membranes. The SiC–P and SiC-G membrane surfaces are similar showing sand dune-like surface structures with relatively low roughness degree, while clear valleys and gullies were observed on the SiC-25, SiC-50 and SiC-75 membrane surfaces. It was found that the three SiC membranes with ZnO NS modification showed higher average roughness (Ra) and root mean square roughness (Rq) values than that of SiC–P and SiC-G membrane. This can be ascribed to the deposition of ZnO NSs on the composite membranes, which is consistent with the aforementioned SEM results. We can deduce that more ZnO NSs were locally and anisotropically stacked onto the SiC grains, resulting in an increase of roughness degree.

To further study the surface chemical compositions of SiC-25, SiC-50 and SiC-75 membrane surfaces, XPS tests were conducted. Fig. 5a shows the wide scan XPS spectra of the three membranes surfaces. Under the same testing conditions, the three membrane surfaces exhibited the identical characteristic peaks. The peaks centered at binding energies of about 284.8, 532.0, 102.7 eV correspond to the C1s, O1s, and Si2p, respectively. In addition to the three peaks, Zn2p, ZnLMN, Zn3s and Zn3p peaks [34] were also found in the three membranes, which confirms that the same ZnO NSs were deposited on the membrane surfaces. It is clear that the SiC-75 membrane exhibited the highest relative intensity for Zn-related peaks, which suggests that more ZnO NSs were formed on the SiC-75 membrane surface in comparison with the other two membranes. The Zn2p peak appeared at binding energies of 1021.9–1065.3 eV in the XPS spectra, which was used to reflect Zn elemental content in the total chemical compositions of the three membranes. The atomic ratios of Zn2p for SiC-25, SiC-50 and SiC-75 membranes were 4.74, 6.04 and 6.67%, respectively (Fig. 5b). These results quantitatively confirm that the density of ZnO NSs for the three membrane increases as the precursor concentration increases.

3.2. Surface wettability

Surface wettability of a membrane plays a crucial role in the separation of special oil-water systems [35], thus the surface wettability of the SiC membranes was studied. The pristine SiC and ZnO-deposited SiC membranes without surface grafting with n-octyltriethoxysilane were intrinsically hydrophilic, and no observable static water CAs (WCAs) could be captured for these membranes. Fig. S3 shows the dynamic WCAs of SiC–P, SiC-25, SiC-50 and SiC-75 membranes without surface grafting. The SiC–P membrane exhibited good hydrophilicity that an initial WCA of 40.0° was observed on the surface and the water droplet could permeate into the membrane within 2.5 s. We found the ZnO-deposited SiC membranes were much more hydrophilic than the pristine. The SiC-50 and SiC-75 membranes showed a much stronger affinity toward water molecules and the dropped water droplets on their surfaces rapidly disappeared within about 0.5 s. This result suggests that the introduction of ZnO NSs onto SiC grains efficiently increases the amount of OH groups on the hierarchically composite surfaces.

Fig. S4a shows the static WCAs and oil CAs (OCAs) of the SiC–P, SiC-G, SiC-25, SiC-50 and SiC-75 membranes. No measurable WCA and OCA could be observed for the SiC–P membrane, which suggests that the pristine SiC membrane surface exhibited both hydrophilicity and oleophilicity. In contrast, the simply grafted SiC membranes (SiC-G) were hydrophobic with a WCA of 134.2 ± 3.4°, which agrees with previous reports [36]. No observable static OCA was found for SiC-G membranes, indicating that n-octyltriethoxysilane-grafted SiC membranes exhibited excellent oils (e.g. hexane) affinity. For the ZnO-deposited SiC membranes with surface grafting, the WCAs of SiC-25, SiC-50 and SiC-75 membranes were 147.0 ± 4.5°, 166.4 ± 3.2° and 174.4 ± 4.6°, respectively. In addition, no static OCAs (i.e. 0°) could be measured for those membranes. In addition, we also found both SiC-50 and SiC-75 membrane surfaces exhibited sliding angles below 10° (Fig. S5). Therefore, according to the commonly accepted definition of a superhydrophobic-superoleophilic surface [37], the SiC-50 and SiC-75 membranes were superhydrophobic-superoleophilic.

Fig. S6 demonstrates the water and oil contacting experiments on the SiC membrane surfaces. The photos of the SiC membrane surfaces before and after adding 20 μL water (blue) or oil (red) droplets were recorded. Once dropping a blue water or a red oil droplet onto the SiC membrane surfaces, both water and oil droplets could rapidly spread and penetrate the SiC–P membrane. However, only red oil droplets could penetrate

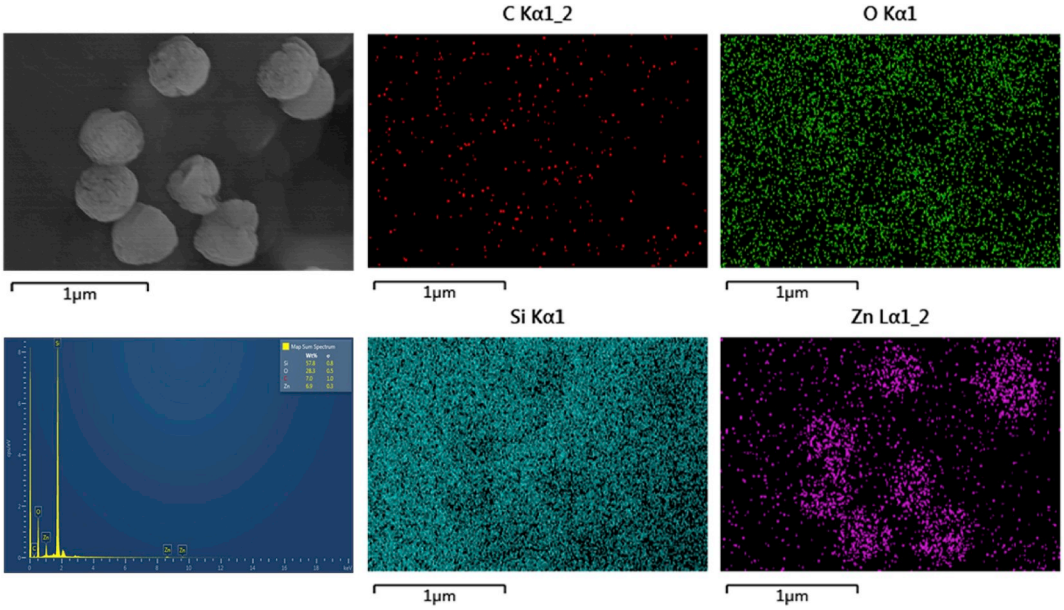

Fig. 3. EDS spectra and elemental mappings of the SiC-50 membrane surface.

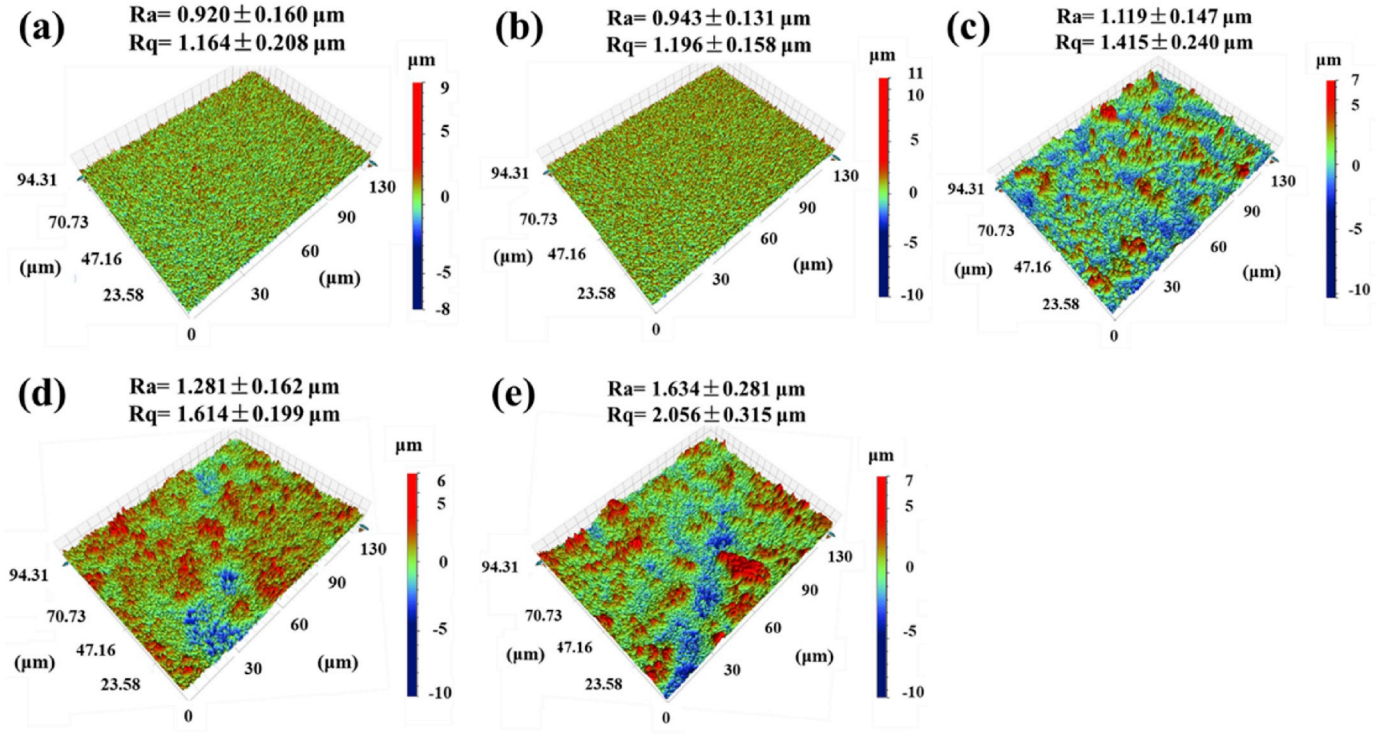

Fig. 4. Three-dimensional (3D) surface profiles of the (a) SiC–P, (b) SiC-G, (c) SiC-25, (d) SiC-50 and (e) SiC-75 membranes.

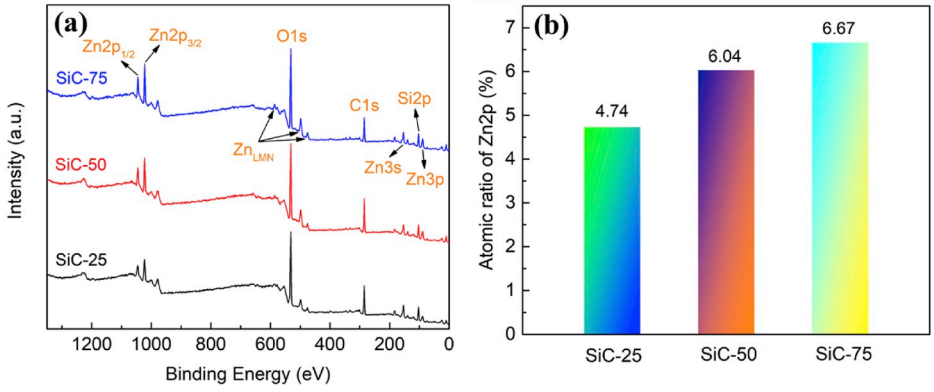

Fig. 5. XPS analysis of the ZnO-deposited SiC membranes: (a) wide-scan; (b) atomic ratio of Zn2p.

SiC-G, SiC-25, SiC-50 and SiC-75 membranes, blue water droplets were observed on these membrane surfaces. After removal of the blue droplets on these membranes using clean wipes via capillary force, obvious blue traces could be found on the SiC-G surface. Faint blue traces were observed in the SiC-25 sample, but no blue traces could be observed on SiC-50 and SiC-75 membrane surfaces. These results are consistent with the above-mentioned static CA analysis and suggest that SiC-50 and SiC-75 membrane could completely repel water molecules.

To further study the oleophilicity, dynamic OCAs of the SiC membranes were measured. In Fig. S7, when dropping 5 μL hexane onto the pristine SiC membrane, an initial CA of 16.3° was observed and the CA could disappear within 0.37 s. The initial OCA for the SiC-25 membrane was a little higher than that of SiC-G, but the oil droplet could penetrate the SiC-25 membrane faster than for the SiC-G membrane. SiC-75 membrane surface displayed a low initial OCA of 7.5° but the OCA lasted about 0.22 s until disappearance. Moreover, the SiC-50 membrane exhibited the lowest initial OCA of 4.5° and the OCA became 0° within the shortest time (~0.07 s). The surface free energies of the five SiC membrane surfaces are given in Table 1. The total surface free energies of SiC–P and SiC-G membranes were 51.9 and 38.1 mN m^{-1}, respectively, indicating the silane grafting could effectively lower the surface free energy of SiC membranes. Notably, all the SiC membranes with ZnO NS modification and silane grafting exhibited extremely low surface free energies, which confirms that the rough hierarchical ZnO–SiC structures are easy to achieve much lower surface free energy after grafting with

Table 1
Surface free energies of SiC–P, SiC-G, SiC-25, SiC-50 and SiC-75 membranes.

Ceramic membranes	Contact angle/°		Surface free energy/mN·m^{-1}		
	Ethylene glycol	Diiodo-methane	Dispersive component	Non-Dispersive component	Total
SiC	20.0	8.0	44.50	7.39	51.9
SiC-G	58.0	42.0	35.40	2.68	38.1
SiC-25	104.4	100.4	9.76	8.53	1.23
SiC-50	120	100	6.92	8.67	-1.75
SiC-75	125	100.9	6.01	8.35	-2.34

silane.

3.3. Evaluation of w/o emulsion separation performance

To evaluate the w/o emulsion separation performance of the SiC membranes, cross-flow filtration experiments were conducted. As shown in Fig. 6, the changes of instant oil flux for SiC–P, SiC-G, SiC-25, SiC-50 and SiC-75 membranes varying with operation time were monitored. The same feed w/o emulsion (500 ppm water-in-hexane) with mean water droplet diameter of ~320 nm (Fig. S8a) and the constant transmembrane pressure (1 bar) were applied. The initial oil flux of the SiC–P membrane was 1201.21 L m^{-2} h^{-1}·bar^{-1}, which was similar to that of the SiC-G membrane. The instant oil fluxes of SiC–P and SiC-G membrane decreased drastically in the first 20 min and then reached a steady-state, and the former was always about 2–3 times slower than the later, suggesting that the hydrophobic SiC-G membrane showed higher oil flux than the hydrophilic SiC–P membrane under same operational conditions. Notably, the initial oil fluxes of SiC-25, SiC-50 and SiC-75 membranes were similar which were a little higher than SiC membranes without ZnO NSs deposition, and the oil flux decline tendencies for SiC-25, SiC-50 and SiC-75 membranes were significantly alleviated. Among the three ZnO-deposited membranes, SiC-50 membrane showed the highest initial oil flux of 1325.99 L m^{-2} h^{-1} and its instant oil flux became stable after 35 min with the values between 971.26 and 1010.12 L m^{-2} h^{-1}. The trends of oil flux for SiC-25 and SiC-50 membranes were similar and their oil fluxes at the operation time of 60 min were 718.49 and 747.31 L m^{-2} h^{-1}, respectively. For the rejection of these membranes, all the filtrates of the five SiC membranes were clean in appearance. However, the filtrate of the SiC–P membrane had the detectable droplets and the size of the droplets became smaller compared with the feed (Fig. S8b), while no droplets were found in the filtrates of the SiC-G, SiC-25, SiC-50 and SiC-75 membranes. Combined with optical microscope analysis, the rejections of SiC–P and SiC-G membrane were about 85% and 95%, respectively, which indicates that hydrophobic modification could improve w/o emulsion separation efficiency for ceramic membranes in terms of both oil flux and rejection. In addition, all the SiC-25, SiC-50 and SiC-75 exhibited unique rejection performance that they could completely reject water droplets (i.e. R = ~99%, Fig. S9).

In fact, it is well known that the major challenge in w/o emulsion separation process is the membrane pore plugging caused by water droplets leads to diminished oil flux [6]. Understanding the water-repellency mechanism is of great importance. In our case, hexane with low viscosity tends to first pass through the SiC membrane surface rapidly and the rejected water droplets accumulated on the membrane surface forming a barrier layer that results in the flux decline. We believe the alleviated oil flux decline mechanism for the SiC-25, SiC-50 and SiC-75 membranes can be ascribed to the synergetic effects of their micro-nano hierarchical structures and special wettability. According to Cassie-Baxter's theory [38], the anti-wetting states could be tuned from Cassie state via metastable state to Wenzel state [39] and the precisely tailored hierarchical structure could reduce the area fraction for water droplets. In addition, the ZnO NS deposition degree is also proportional to membrane transport resistance. For example, the superhydrophobicity-superoleophilicity of the SiC-50 membrane could quickly attract hexane and prevent water droplets from contacting the hierarchical structure to avoid the membrane surface from the formation of a water layer. The appropriated ZnO NS deposition degree of the SiC-50 membrane did not increase much resistance to hexane. Therefore, under the same chemical composition, the relatively moderate structure of the SiC-50 membrane led to its optimal performance in our experiment.

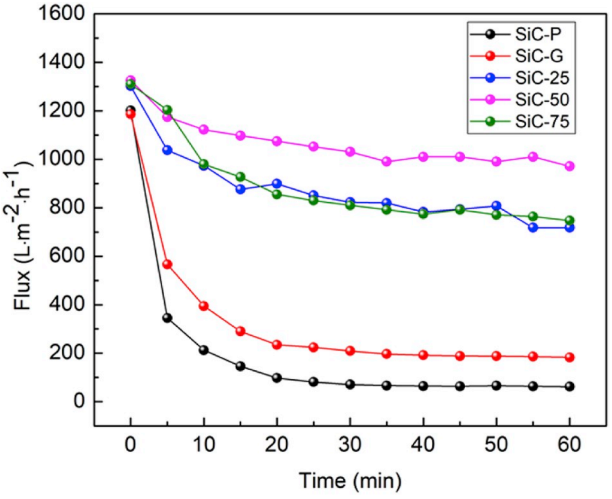

Fig. 6. The oil flux evolutions of the SiC–P, SiC-G, SiC-25, SiC-50 and SiC-75 membranes with filtration time for 500 ppm water-in-hexane emulsion under transmembrane pressure of 1 bar.

Fig. 7 shows the separation performance of the SiC membranes for water-in-hexane emulsions with concentrations of 500 ppm, 1000 ppm and 2000 ppm in terms of their initial oil fluxes, the oil fluxes at the operation time of 60 min (i.e. steady-state oil flux) and the rejection rates for each test. We found that the SiC membranes showed a similar trend in oil flux and rejection for 1000 ppm and 2000 ppm emulsions, compared with their separation performance for 500 ppm emulsion. All the SiC membranes with ZnO NS deposition (i.e. SiC-25, SiC-50 and SiC-75) exhibited higher initial oil fluxes than that of the pristine and the simply grafted SiC membranes (i.e. SiC–P and SiC-G), and the initial oil fluxes of the five types of SiC membranes became lower when treating the w/o emulsion with a higher water content. Although oil flux decline occurred for the five SiC membranes when treating the three w/o emulsions, the stable oil fluxes of SiC-25, SiC-50 and SiC-75 membranes were always much higher than that of SiC–P and SiC-G membranes, indicating that the water-repellency of SiC membranes are efficiently improved by their micro-nano hierarchically ZnO–SiC structures and the special wettability. Moreover, the SiC-50 membranes showed the best separation performance for all the three emulsions, further proving its structural superiority for w/o emulsion separation.

Table 2 compares w/o emulsion separation performance of the SiC-50 membrane with that of other reported hydrophobic ceramic membranes. As mentioned above, silane grafting is commonly used for changing hydrophilic ceramic membrane materials with high hydrophobicity. Gao et al. modified a ZrO_2 membrane using hexadecyltrimethoxysilane (HDTMS) as grafting reagent and investigated the performance of the modified membrane in water-in-kerosene system separation [11,18]. They found that hydrophobic modification is very efficient for alleviating the oil flux decline of the pristine ZrO_2 membranes and the modified membranes exhibited a steady-state flux of 400–620 L m^{-2} h^{-1} under transmembrane pressure of 1 bar and a rejection of ~99.0% to the separation system. The same group also modified Al_2O_3 membranes using HDTMS for separating other w/o emulsions [35]. For water-in-hexane emulsion, the hydrophobic Al_2O_3 membrane with the pore size of 1 μm could display a steady-state flux of 1025 L m^{-2} h^{-1} under transmembrane pressure of 1 bar and completely reject water content (i.e. R = 99.0%). However, these hydrophobic ceramic membranes are not superhydrophobic-superoleophilic and severe oil flux decline was still found in the separation processes.

Ahmad et al. [25] developed a superhydrophobic Al_2O_3 microfiltration (MF) membrane by grafting fuoroalkylsilane (FAS) on the sol-gel pre-coated membrane surface for water-in-kerosene separation. Their membrane also showed excellent rejection to water but the flux was approximately 400 L m^{-2} h^{-1} under 1 bar. Su et al. [24] reported a porous ceramic membrane with a superhydrophobic-superoleophilic surface for reclaiming kerosene from water–kerosene–clay water mixture. A commercial porous ceramic tube was first coated with a tetraethoxysilane (TEOS)-derived silica sol and then the membrane

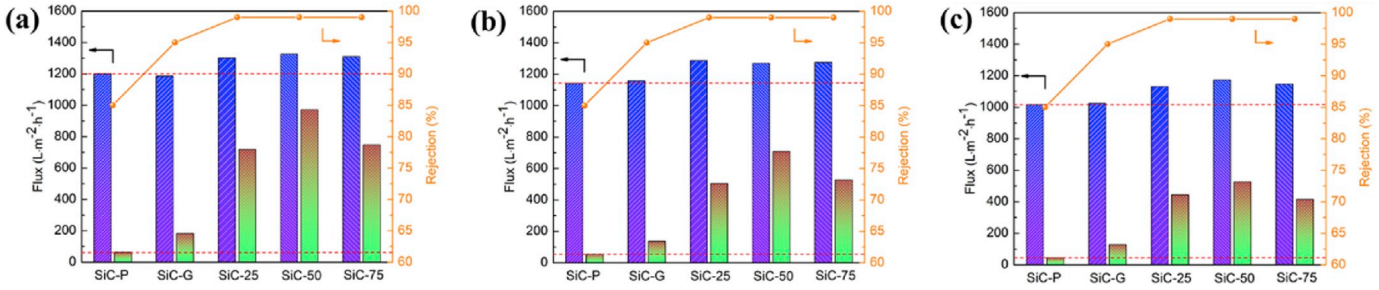

Fig. 7. Initial and stable oil fluxes and rejections of SiC–P, SiC-G, SiC-25, SiC-50 and SiC-75 membranes for (a) 500 ppm w/o emulsion, (b) 1000 ppm w/o emulsion and (c) 2000 ppm w/o emulsion under transmembrane pressure of 1 bar.

Table 2
Comparison of the optimal membrane in this work with other reported hydrophobic ceramic membranes in terms of w/o emulsion separation.

Membrane	PS (μm)	WCA (°)	System	J (LHM)	R (%)	Ref
ZrO_2-HDTMS	0.2	134.0	w/k	400–620	98.8	[11,18]
Al_2O_3-HDTMS	1	135.7	w/h	~1025	99.0	[35]
Al_2O_3-HDTMS	1	135.7	w/i	~955	99.0	[35]
Al_2O_3-HDTMS	1	135.7	w/p	~1911	99.0	[35]
Al_2O_3-FAS	0.35	158.4	w/k	~400	99.9	[25]
Ceramic-PDMS	30	161.2	w/k	n.a.	67.6	[24]
SiC-50	0.25	167.0	w/h	~1000	99.0	This work

Abbreviations: PS, pore size; LHM, $L{\cdot}m^{-2}{\cdot}h^{-1}$; w/k, water-in-kerosene; w/h, water-in-hexane; w/i, water-in-isooctane; w/p, water-in-phenixin; n.a., not available.

surface was coated with a polyurethane-polydimethylsiloxane (PU-PDMS) film. The resulting ceramic membrane showed a WCA of 161.2° and a kerosene OCA of 0°, and the optimal kerosene recovery efficiency was 67.6%. Unfortunately, the authors did not provide sufficient information on oil flux. We note that all these hydrophobic ceramic membranes exhibit excellent rejection to water and their oil fluxes depend on the membrane (e.g. pore size and wettability) and the w/o emulsion system (e.g. concentration of water content and viscosity of oil). Therefore, the steady-state flux and flux decline ratio are two crucial factors to evaluate the performance of a membrane in a certain w/o emulsion separation process. In this work, the superhydrophobic-superoleophilic SiC-50 membrane shows excellent w/o emulsion separation efficiency with relatively high steady-state flux and low flux decline ratio, which makes it very competitive when applied to remove water content from w/o emulsions.

3.4. Stability of superhydrophobicity

The stability of the superhydrophobic-superoleophilic SiC membranes, in essence, is the stability of their superhydrophobicity. The static WCAs of the SiC-G and SiC-75 membrane surfaces were compared after exposing the membranes in the air or immersing the membranes in hexane, petroleum ether and 260# solvent oil for 30 days (Fig. 8). We observed that the WCAs of the two membranes nearly remained at their initial value when exposed to air, soaked in hexane, petroleum ether and 260# solvent oil after 30 days. All WCAs of SiC-75 membrane obtained after the 30-day test were still higher than 150°. These results demonstrate that our superhydrophobic SiC membranes are stable in different oils and they may be used for removing water content from various w/o emulsions.

4. Conclusions

In summary, superhydrophobic-superoleophilic SiC membranes with

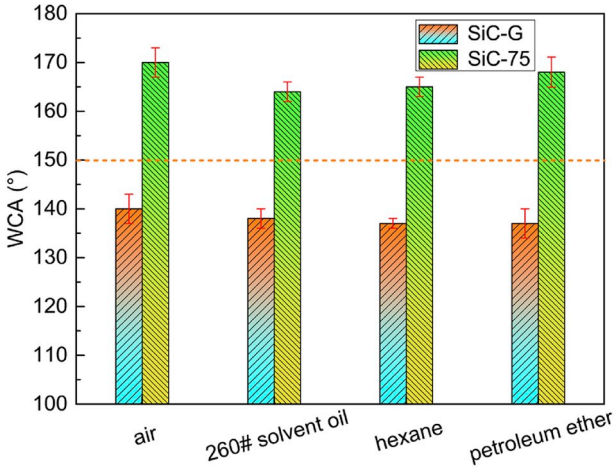

Fig. 8. WCAs of the SiC-G and SiC-75 membrane surfaces when exposed in air, soaked in 260# solvent oil, soaked in hexane and soaked in petroleum ether after 30 days.

tunable micro-nano hierarchical structures were successfully fabricated by chemical solution deposition of ZnO NSs and post-modification with n-octyltriethoxysilane. The density of ZnO NSs on SiC membrane surfaces increases as the Zn^{2+} precursor concentration increases. When the concentration of Zn^{2+} is above 50 mM, the SiC membrane could become superhydrophobic. Compared with the pristine and simply grafted membranes, all the SiC membranes with ZnO NS and n-octyltriethoxysilane modification exhibited significantly improved efficiency in terms of oil flux and water rejection when treating water-in-hexane emulsions. The SiC-50 membrane displayed the optimal performance with steady-state oil flux of ~1000 L m^{-2} h^{-1} under 1 bar and water rejection of ~99% for 500 ppm water-in-hexane emulsion, and the corresponding water-repellency mechanism was revealed. Moreover, compared with reported hydrophobic ceramic membranes for w/o emulsion separation, our SiC-50 membrane is extremely competitive. The stability of superhydrophobicity for the SiC-75 membrane in air and different oils was also confirmed. This study provides a simple method for developing superhydrophobic-superoleophilic ceramic membranes and demonstrates that superhydrophobic modification of ceramic membranes is effective for improving their efficiency in removing water content from oil products.

Declaration of competing interestCOI

The authors declare that they have no known competing financial interests or personal relationships that could have appeared to influence the work reported in this paper.

CRediT authorship contribution statement

Yibin Wei: Conceptualization, Methodology, Investigation, Formal analysis, Writing - original draft. **Zixuan Xie:** Investigation, Formal analysis, Validation, Writing - review & editing. **Hong Qi:** Investigation, Supervision, Writing - review & editing, Funding acquisition.

Acknowledgments

This work is supported by the National Natural Science Foundation of China of China (21490581), China Petroleum & Chemical Corporation (317008-6) and Guangxi Innovation Driven Development Foundation.

Appendix A. Supplementary data

Supplementary data to this article can be found online at https://doi.org/10.1016/j.memsci.2020.117842.

References

[1] Z. Chu, Y. Feng, S. Seeger, Oil/water separation with selective superantiwetting/superwetting surface materials, Angew. Chem. Int. Ed. 54 (2015) 2328–2338.
[2] M. Padaki, R. Surya Murali, M.S. Abdullah, N. Misdan, A. Moslehyani, M.A. Kassim, N. Hilal, A.F. Ismail, Membrane technology enhancement in oil–water separation. A review, Desalination 357 (2015) 197–207.
[3] W. Zhang, N. Liu, Y. Cao, X. Lin, Y. Liu, L. Feng, Superwetting porous materials for wastewater treatment: from immiscible oil/water mixture to emulsion separation, Adv. Mater. Interfaces (2017), 1600029.
[4] Y. Zhu, D. Wang, L. Jiang, J. Jin, Recent progress in developing advanced membranes for emulsified oil/water separation, NPG Asia Mater. 6 (2014), e101.
[5] E.N. Tummons, V.V. Tarabara, Jia W. Chew, A.G. Fane, Behavior of oil droplets at the membrane surface during crossflow microfiltration of oil–water emulsions, J. Membr. Sci. 500 (2016) 211–224.
[6] Y. Wei, H. Qi, X. Gong, S. Zhao, Specially wettable membranes for oil-water separation, Adv. Mater. Interfaces 5 (2018) 1800576.
[7] D. Lu, T. Zhang, J. Ma, Ceramic membrane fouling during ultrafiltration of oil/water emulsions: roles played by stabilization surfactants of oil droplets, Environ. Sci. Technol. 49 (2015) 4235–4244.
[8] L. Zhu, X. Dong, M. Xu, F. Yang, M.D. Guiver, Y. Dong, Fabrication of mullite ceramic-supported carbon nanotube composite membranes with enhanced performance in direct separation of high-temperature emulsified oil droplets, J. Membr. Sci. 582 (2019) 140–150.
[9] L. Cot, C. Guizard, A.L.A. Julbe, Preparation and Application of Inorganic Membranes, 1994.
[10] S. Munirasu, M.A. Haija, F. Banat, Use of membrane technology for oil field and refinery produced water treatment—a review, Process Saf. Environ. Prot. 100 (2016) 183–202.
[11] N. Gao, M. Li, W. Jing, Y. Fan, N. Xu, Improving the filtration performance of ZrO2 membrane in non-polar organic solvents by surface hydrophobic modification, J. Membr. Sci. 375 (2011) 276–283.
[12] B.R. Solomon, N. Hyder, K.K. Varanasi, Separating oil-water nanoemulsions using flux-enhanced hierarchical membranes, Sci. Rep. 4 (2014).
[13] S.S. Madaeni, S. Zinadini, V. Vatanpour, Preparation of superhydrophobic nanofiltration membrane by embedding multiwalled carbon nanotube and polydimethylsiloxane in pores of microfiltration membrane, Separ. Purif. Technol. 111 (2013) 98–107.
[14] N.A. Ahmad, C.P. Leo, A.L. Ahmad, W.K.W. Ramli, Membranes with great hydrophobicity: a review on preparation and characterization, Separ. Purif. Rev. 44 (2015) 109–134.
[15] J. Kujawa, W. Kujawski, A. Cyganiuk, L.F. Dumée, S. Al-Gharabli, Upgrading of zirconia membrane performance in removal of hazardous VOCs from water by surface functionalization, Chem. Eng. J. 374 (2019) 155–169.
[16] J. Kujawa, S. Cerneaux, W. Kujawski, Highly hydrophobic ceramic membranes applied to the removal of volatile organic compounds in pervaporation, Chem. Eng. J. 260 (2015) 43–54.
[17] S. Wang, L. Jiang, Definition of superhydrophobic states, Adv. Mater. 19 (2007) 3423–3424.
[18] N. Gao, Y. Fan, X. Quan, Y. Cai, D. Zhou, Modified ceramic membranes for low fouling separation of water-in-oil emulsions, J. Mater. Sci. 51 (2016) 6379–6388.
[19] J.M. Dickhout, J. Moreno, P.M. Biesheuvel, L. Boels, R.G. Lammertink, W.M. de Vos, Produced water treatment by membranes: a review from a colloidal perspective, J. Colloid Interface Sci. 487 (2017) 523–534.
[20] B. Su, Y. Tian, L. Jiang, Bioinspired interfaces with superwettability: from materials to chemistry, J. Am. Chem. Soc. 138 (2016) 1727–1748.
[21] K. Yin, H. Du, X. Dong, C. Wang, J.A. Duan, J. He, A simple way to achieve bioinspired hybrid wettability surface with micro/nanopatterns for efficient fog collection, Nanoscale 9 (2017) 14620–14626.
[22] Y. Long, Y. Shen, H. Tian, Y. Yang, H. Feng, J. Li, Superwettable Coprinus comatus coated membranes used toward the controllable separation of emulsified oil/water mixtures, J. Membr. Sci. 565 (2018) 85–94.
[23] Z. Wang, W. Kong, L. Si, J. Niu, Y. Liu, L. Yin, Z. Tian, Robust and thermally stable butterfly-like Co(OH)2/Hexadecyltrimethoxysilane superhydrophobic mesh filters prepared by electrodeposition for highly efficient oil/water separation, Ind. Eng. Chem. Res. 58 (2019) 9576–9584.
[24] C. Su, Y. Xu, W. Zhang, Y. Liu, J. Li, Porous ceramic membrane with superhydrophobic and superoleophilic surface for reclaiming oil from oily water, Appl. Surf. Sci. 258 (2012) 2319–2323.
[25] N.A. Ahmad, C.P. Leo, A.L. Ahmad, Superhydrophobic alumina membrane by steam impingement: minimum resistance in microfiltration, Separ. Purif. Technol. 107 (2013) 187–194.
[26] J. Lu, Y. Yu, J. Zhou, L. Song, X. Hu, A. Larbot, FAS grafted superhydrophobic ceramic membrane, Appl. Surf. Sci. 255 (2009) 9092–9099.
[27] Y. Dong, L. Ma, C.Y. Tang, F. Yang, X. Quan, D. Jassby, M.J. Zaworotko, M. D. Guiver, Stable superhydrophobic ceramic-based carbon nanotube composite desalination membranes, Nano Lett. 18 (2018) 5514–5521.
[28] G. Kwon, E. Post, A. Tuteja, Membranes with selective wettability for the separation of oil–water mixtures, MRS Commun. 5 (2015) 475–494.
[29] Y. Peng, Z. Guo, Recent advances in biomimetic thin membranes applied in emulsified oil/water separation, J. Mater. Chem. 4 (2016) 15749–15770.
[30] M. Kokotov, G. Hodes, Reliable chemical bath deposition of ZnO films with controllable morphology from ethanolamine-based solutions using KMnO4 substrate activation, J. Mater. Chem. 19 (2009) 3847.
[31] A. Huang, L.-H. Chen, C.-C. Kan, T.-Y. Hsu, S.-E. Wu, K.K. Jana, K.-L. Tung, Fabrication of zinc oxide nanostructure coated membranes for efficient oil/water separation, J. Membr. Sci. 566 (2018) 249–257.
[32] S. Wu, Polar and nonpolar interactions in adhesion, J. Adhes. 5 (1973) 39–55.
[33] C.J. Vanoss, R.F. Giese, The hydrophilicity and hydrophobicity of clay-minerals, Clay Clay Miner. 43 (1995) 474–477.
[34] B. Xu, Z. Cai, Fabrication of a superhydrophobic ZnO nanorod array film on cotton fabrics via a wet chemical route and hydrophobic modification, Appl. Surf. Sci. 254 (2008) 5899–5904.
[35] D. Ding, H. Mao, X. Chen, M. Qiu, Y. Fan, Underwater superoleophobic-underoil superhydrophobic Janus ceramic membrane with its switchable separation in oil/water emulsions, J. Membr. Sci. 565 (2018) 303–310.
[36] X. Li, Y. Wei, Z. Xie, H. Qi, Hydrophobic modification of Al2O3 and SiC microfiltration membranes for oil-solid separation, CIESC J. 70 (2019) 2737–2747.
[37] J. Drelich, E. Chibowski, Superhydrophilic and superwetting surfaces: definition and mechanisms of control, Langmuir 26 (2010) 18621–18623.
[38] A. Cassie, S. Baxter, Wettability of porous surfaces, Trans. Faraday Soc. 40 (1944) 546–551.
[39] J. Li, Z. Jing, F. Zha, Y. Yang, Q. Wang, Z. Lei, Facile spray-coating process for the fabrication of tunable adhesive superhydrophobic surfaces with heterogeneous chemical compositions used for selective transportation of microdroplets with different volumes, ACS Appl. Mater. Interfaces 6 (2014) 8868–8877.